Evolution of Tribological Properties of Cast Al–10Zn–2Mg Alloy Subjected to Severe Plastic Deformation

G. K. Manjunath, G. V. Preetham Kumar and K. Udaya Bhat

Abstract In the current investigation, tribological behaviour of the cast Al–10Zn–2Mg alloy processed by severe plastic deformation (SPD) technique was studied. In this work, one of the SPD techniques, equal channel angular pressing (ECAP) was adopted as a processing tool. ECAP was carried out in route B_C and processing was attempted at the lowest temperature. After ECAP, grain structure of the material was refined and considerable improvement in the microhardness of the alloy was perceived. Mainly, wear resistance of the alloy material was enhanced with successive ECAP passes. Coefficient of friction of the alloy material was decreased with successive ECAP passes. Wear resistance of the alloy was decreased with a rise in the applied load and the sliding speed. Both at low and high load condition, abrasive wear was noticed in as-cast and homogenized specimens. Whereas in ECAPed specimens, in addition to abrasive wear, oxidation wear and adhesive wear were observed in low load and it changes to abrasive wear at high load. In the ECAPed specimens, at low load transfer of iron particles from the steel disc surface to the specimen surface was identified.

Keywords Wear · Al–Zn–Mg alloy · SPD · ECAP · Wear mechanism

G. K. Manjunath · G. V. Preetham Kumar · K. Udaya Bhat (✉)
Department of Metallurgical and Materials Engineering, National Institute of Technology Karnataka, Srinivasnagar P.O., Surathkal, Mangalore 575025, India
e-mail: udayabhatk@gmail.com

G. K. Manjunath
e-mail: manjugk2001@gmail.com

G. V. Preetham Kumar
e-mail: pkphd@hotmail.com

R. V. Prakash et al. (eds.), *Structural Integrity Assessment*, Lecture Notes in Mechanical Engineering, https://doi.org/10.1007/978-981-13-8767-8_13

1 Introduction

Aluminium alloys are considered as a reliable material in the field of engineering applications. The Al–Zn–Mg alloys are acknowledged as the hardest and strongest alloys amongst aluminium alloys family [1]. Al–Zn–Mg alloys have earned wide appreciation in the development of lightweight equipment where high strength to weight ratio is an essential criterion [2]. However, poor ductility and low wear resistance of these alloys in cast condition obstruct its utilization in industries. Wear is identified as an important property in the design and manufacture of engineering equipment. Wear resistance capability of a material can be enhanced by strengthening the material [3]. Strength of the material can be enhanced by grain refinement through various severe plastic deformation (SPD) techniques. Among various SPD techniques, equal channel angular pressing (ECAP) is more attractive because of its simplicity [4]. ECAP was first introduced in 1972 by Segal, later during the 1990s, this process gained attention to develop ultra-fine-grained materials [5]. In ECAP process, the specimen is pushed through two channels which are intersecting at an angle (Φ). Large volume of shear strain is generated in the specimen as it crosses the intersecting line of two channels, which in turn causes grain size to decrease considerably along with the generation of large amount dislocations. The speciality of the ECAP is that after processing, the cross section of the specimen is unchanged so the same specimen could be processed repetitively to achieve higher grain refinement [6].

Numerous literature were reported on the implementation of the SPD process to Al–Zn–Mg alloys, particularly to identify the impact of the SPD process on the mechanical properties and evolution of microstructure [7–9]. In spite of that, wear study of the Al–Zn–Mg alloys processed by SPD techniques have not gained much consideration. In order to get optimal usage of the SPD processed alloys and materials, it is required to study the tribological properties of these materials. Since UFG materials processed by SPD techniques possess high strength and hardness [10]. They are expected to have good wear resistance. From the limited available literature on the tribological behaviour of the SPD processed materials, both favourable and unfavourable effects were observed [11]. So it is necessary to study the effect of ECAP on the tribological properties of Al–Zn–Mg alloys. It is very interesting to investigate the tribological performance of the SPD processed Al–Zn–Mg alloys. In this regard, in the present work, tribological properties of the ECAP processed cast Al–10Zn–2Mg alloy was studied and the consequence of ECAP on the tribological behaviour of the material was investigated. The composition of the material selected in the current investigation closely matches the composition of the Al 7034 alloy. This alloy is presently used in the fabrication of the lightweight structures [12].

2 Experimental

The material studied in the current investigation was prepared through a gravity casting technique. The procedure for the specimen preparation by gravity casting technique is described in our previous report [13]. The composition of the cast material was checked through optical emission spectroscopy (OES). Results obtained through OES technique is presented in Table 1. As-cast material was treated with a homogenization process at 753 K for 20 h. For ECAP, homogenized material was machined to Ø 15.9 mm and 80 mm height rods. The ECAP was carried out in a split die having channel diameter of 16 mm. The channels of the die are interconnecting at an angle (Φ) of 120º and having an external arc of curvature (Ψ) of 30º. With these angles, in each pass, a stain of 0.667 is imposed on the specimen. ECAP was attempted to carry out at the lowest possible temperature in route B_C and at a speed ≈ 0.5 mm/sec. Molybdenum disulphide was coated on the specimen surface and in the die channels to control friction during processing. A separate heating arrangement was used for heating the die assembly to the necessary temperature and the same temperature is retained while processing.

Microstructure of the specimens was studied by using scanning electron microscope (SEM) and energy dispersive spectroscopy (EDS) was carried out to check the chemical composition of the precipitates. For microstructural study, the specimens were polished using a sequence of silicon carbide abrasive papers followed by cloth polishing using aluminium oxide particles and distilled water. Lastly, specimens were etched using Keller's reagent. Microhardness was measured by using Vickers microhardness tester. The Vickers microhardness (Hv) was obtained by imposing a load of 50 gm for 15 s. Dry sliding wear tests were conducted in pin on disc arrangement at ambient temperature. To carry out wear tests, processed and unprocessed specimens were machined to cylindrical pins of Ø10 mm and 28 mm height. Specimens were made to slide against EN31 steel disc having a hardness of 62 HRc. Prior to wear test, specimen and the disc were washed with acetone. To investigate the wear resistance capability of the alloy material, wear tests were conducted at different loads and sliding speeds. These conditions are presented in Table 2. In all conditions, wear tests were done for a span of 1000 m and in a circular track of Ø 120 mm. The wear resistance was measured by weight loss method.

Table 1 Composition the material verified through optical emission spectroscopy

Element	Al	Zn	Mg	Fe	Mn	Si	Zr	Cu	Ti	Ni	Cr	Pb
Weight (%)	87.3	10.1	2.1	0.23	0.074	0.16	0.005	0.022	0.003	0.002	0.002	0.002

Table 2 Wear test conditions

	C1	C2	C3	C4
Load (N)	19.62	19.62	39.24	39.24
Sliding speed (m/s)	1	2	1	2

The coefficient of friction was obtained through frictional force and load data documented in the controller. The surface morphology and the quantitative elemental analysis of the worn surfaces of the specimens were done in SEM.

3 Results and Discussion

The literature on various SPD process indicates that more refined grain structure could be achieved by processing the material at the lowest possible temperature [14]. On this detail, the material was attempted to process at the lowest temperature. Processing was unsuccessful in the first pass itself at room temperature, 373 and 398 K. At 423 and 448 K, the material fruitfully processed in the first pass and they cracked during the second pass in route B_C. At 473 K, the material was fruitfully processed up to four passes in route B_C without crack. This was the lowest possible temperature at which the material might be fruitfully processed in route B_C without fail up to four passes. In this section, results related to the material ECAP processed at 423 and 473 K is presented.

3.1 Microstructure

Figure 1 presents the microstructure of the material in various conditions. In as-cast state, the microstructure is composed of dendrites and the precipitates were

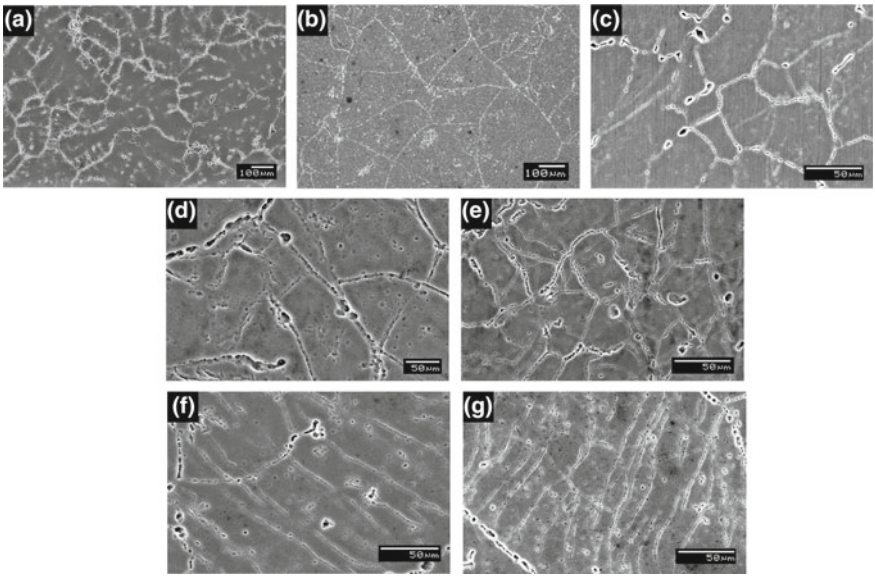

Fig. 1 SEM micrographs of the material **a** as-cast, **b** homogenized, **c** 1 pass at 423 K, **d** 1 pass at 473 K **e** 2 pass at 473 K, **f** 3 pass at 473 K and **g** 4 pass at 473 K

observed in the inter-dendritic spaces as shown in Fig. 1a. Size of the dendrites measured in this condition is approximately equal to 280 μm. The precipitates in the inter-dendritic spaces were identified as η' phase ($MgZn_2$) precipitates [15]. The composition of the precipitates was also confirmed through SEM-EDS analysis. The EDS report is presented in Fig. 2. After homogenization, large-size grains approximately equal to 260 μm replaced the dendritic structure and the precipitates in the inter-dendritic spaces were almost dissolved in the base material as shown in Fig. 1b. After ECAP, grain structure of the material was refined. After one pass ECAP at 423 K, the grain size of the material was approximately decreased to 60 μm as shown in Fig. 1c. Also, precipitates were observed nearby grain boundaries. After ECAP at 473 K, the grain size was decreased to 75 μm in the first pass, 40 μm in the second pass, 20 μm in the third pass and 8 μm in the fourth pass as shown in Fig. 1d, e, f and g, respectively. The detailed investigation of the microstructure evolution after ECAP processing of this material was presented in our earlier work [16, 17]. Figure 3 presents the morphology of the precipitates in the material. In as-cast condition, large flake-shaped precipitates were noticed as

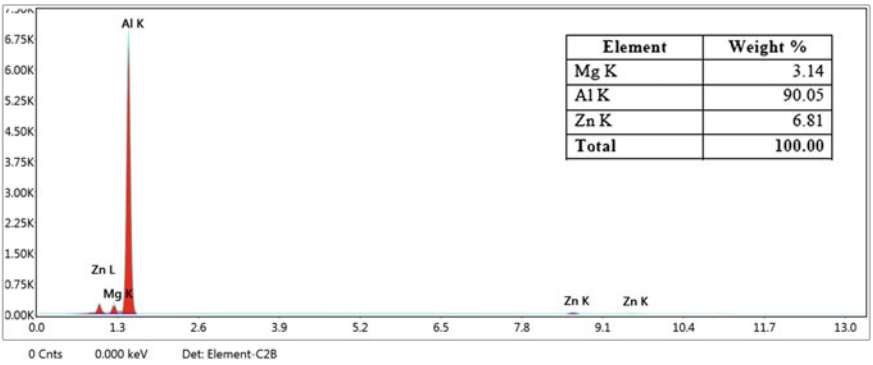

Element	Weight %
Mg K	3.14
Al K	90.05
Zn K	6.81
Total	100.00

Fig. 2 EDS report of the material in as-cast condition

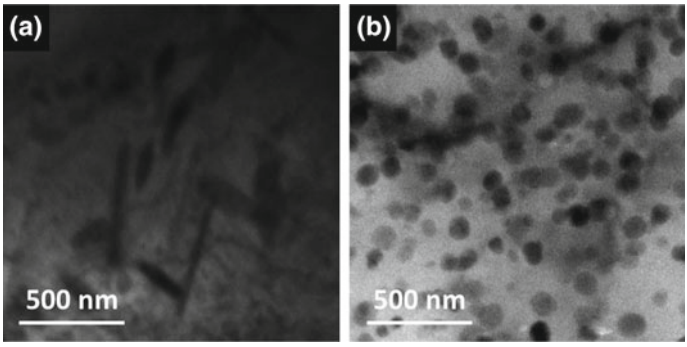

Fig. 3 TEM micrographs of the material **a** as-cast and **b** 4 pass at 473 K

shown in Fig. 3a. After four passes at 473 K, fine spherical-shaped precipitates were noticed. Also, these precipitates were uniformly distributed in the alloy as shown in Fig. 3b.

3.2 Microhardness

Table 3 displays the microhardness of the alloy material in different conditions. In as-cast state, the microhardness of the material is 144 Hv. After homogenization, the microhardness of the alloy material is improved to 155 Hv (8% improvement from the as-cast state). Significant improvement in the microhardness of the material was perceived after ECAP. After one pass ECAP at 423 K, the microhardness of the alloy material was improved to 216 Hv (50% improvement from the as-cast state) [16]. After ECAP at 473 K, the microhardness of the alloy material was enhanced to 204, 223, 232 and 240 Hv in the first, second, third and fourth passes, respectively. After ECAP processing at 473 K, the microhardness was increased by 42, 55, 61 and 67% in the first, second, third and fourth passes, correspondingly from the as-cast state [17]. Improvement in the microhardness of the alloy material after ECAP is owing to the grain refinement, work hardening of the material due to the development of high-density dislocations and formation of high angle grain boundaries [18].

3.3 Wear Properties

3.3.1 Wear Rate

Table 4 displays wear rate of the material in different conditions. The wear rate presented is in the magnitude of 10^{-3} mm^3/m. It is noticed that wear rate is lower in

Table 3 Microhardness (Hv) of the material in different conditions

As-cast	Homogenized	1 pass (423 K)	1 pass (473 K)	2 pass (473 K)	3 pass (473 K)	4 pass (473 K)
144	155	216	204	223	232	240

Table 4 Wear rate of the material in different conditions

	Wear rate (10^{-3} mm^3/m)			
	C1	C2	C3	C4
As-cast	2.169	2.589	3.009	3.394
Homogenized	1.889	2.274	2.799	3.149
1 pass (423 K)	1.365	1.819	2.239	2.589
1 pass (473 K)	1.470	1.924	2.344	2.694
2 pass (473 K)	1.190	1.540	2.064	2.379
3 pass (473 K)	0.945	1.295	1.819	2.169
4 pass (473 K)	0.805	1.120	1.610	1.889

ECAPed specimens in contrast to the as-cast and the homogenized specimens. Also, the wear rate decreased with successive ECAP passes. A decrease in wear rate in the ECAP processed specimens is credited to decrease in the grain size, rise in the microhardness of the alloy material and uniform distribution of the finer size spherical-shaped precipitates in the alloy after ECAP. But, wear resistance of the ECAPed material was decreased with a rise in the load applied and sliding speed. Even though the wear resistance of the ECAPed material was decreased with a rise in the load applied and sliding speed, in all conditions, ECAP processed specimens show superior wear resistance in contrast to the as-cast and the homogenized specimens. The behaviour of increase in the wear resistance of the alloy material after ECAP is consistent with the previous reports on cast Al-7Si material processed by SPD [19]. It was observed that wear rate is comparatively less in one ECAP pass material processed at 423 K in contrast to the one ECAP pass material processed at 473 K. This is owing to the more hardness perceived in the material when processed at 423 K in contrast to the material processed at 473 K.

3.3.2 Coefficient of Friction (μ)

Table 5 displays the coefficient of friction of the material in different conditions. It is noticed that coefficient of friction is lower in ECAP processed specimens in contrast to the as-cast and the homogenized specimens. Also, the coefficient of friction decreased with successive ECAP passes. Decrease in the coefficient of friction in the ECAP processed specimens is attributed to the decrease in the grain size of the material and formation of homogenized microstructure after ECAP processing. But, the coefficient of friction of the ECAPed material increased with a rise in the load and the sliding speed. Even though the coefficient of friction of the ECAPed material increased with a rise in the load and the sliding speed, in all conditions, ECAP processed specimens possess less coefficient of friction in contrast to the as-cast and the homogenized specimens. The behaviour of decrease in the coefficient of friction of the alloy material after ECAP is consistent with the previous reports on aluminium–bronze material processed by SPD [3].

Table 5 Coefficient of friction (μ) of the material in different conditions

	Coefficient of friction (μ)			
	C1	C2	C3	C4
As-cast	0.35	0.4	0.46	0.5
Homogenized	0.33	0.38	0.44	0.48
1 pass (423 K)	0.26	0.31	0.38	0.42
1 pass (473 K)	0.28	0.32	0.4	0.44
2 pass (473 K)	0.25	0.3	0.38	0.42
3 pass (473 K)	0.24	0.29	0.37	0.41
4 pass (473 K)	0.23	0.28	0.36	0.4

3.4 Wear Surface Morphology

Figure 4 displays the SEM micrographs and EDS report of the worn surfaces of the material in different conditions, after wear test conducted at condition C1. The worn surfaces of the as-cast and homogenized samples were comprised of delamination areas and scratches formed due to the separation of the specimen material in the shape of debris, resulting in abrasive wear as shown in Fig. 4a and b. In the EDS report of the as-cast and homogenized specimens, a small trace of oxygen was perceived. But its consequence on the oxide layer growth was not perceived in SEM micrographs. Figure 4c and d shows the worn surface of the material after one pass ECAP at 423 K and 473 K, respectively. It is noticed that in addition to material delamination, scratches and ploughing; at few locations sticking of the worn particles was also observed. Hence, it is presumed that both adhesive and abrasive wear mechanisms were perceived in the first pass specimen processed at 423 K and 473 K, respectively. In the EDS report, the existence of oxygen content was perceived in the adhered debris. The existence of oxygen indicates the oxide layer

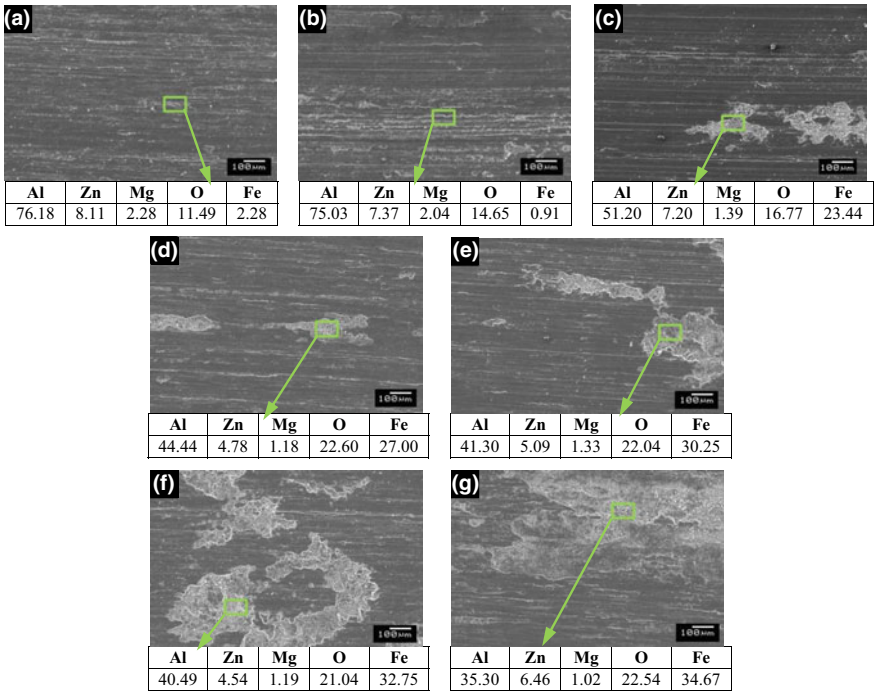

(a) Al	Zn	Mg	O	Fe
76.18	8.11	2.28	11.49	2.28

(b) Al	Zn	Mg	O	Fe
75.03	7.37	2.04	14.65	0.91

(c) Al	Zn	Mg	O	Fe
51.20	7.20	1.39	16.77	23.44

(d) Al	Zn	Mg	O	Fe
44.44	4.78	1.18	22.60	27.00

(e) Al	Zn	Mg	O	Fe
41.30	5.09	1.33	22.04	30.25

(f) Al	Zn	Mg	O	Fe
40.49	4.54	1.19	21.04	32.75

(g) Al	Zn	Mg	O	Fe
35.30	6.46	1.02	22.54	34.67

Fig. 4 SEM micrographs and EDS report of the worn surfaces of the material after wear test conducted at condition C1 **a** as-cast and **b** homogenized**, c** 1 pass at 423 K, **d** 1 pass at 473 K **e** 2 pass at 473 K, **f** 3 pass at 473 K and **g** 4 pass at 473 K (EDS report is collected from the marked area)

growth on the worn surface. Thus, in addition to adhesive and abrasive wear; oxidation wear is too perceived. The presence of iron on the adhered debris indicates that the transfer of the iron elements from the steel disc to the specimen surface. This is owing to the increase in the hardness of the material after ECAP [20]. The adhesion effect is comparatively more in one ECAP pass material processed at 423 K in contrast to the one ECAP pass material processed at 473 K. This is owing to the more hardness perceived in the material when processed at 423 K in contrast to the material processed at 473 K. Figure 4e, f and g show the worn surface of the material after second, third and fourth passses ECAP at 473 K, respectively. It is observed that with successive ECAP passes sticking of the worn particles to the surface of the specimen is increased. Subsequently, delamination and abrasion marks on the worn surfaces were decreased with successive ECAP passes. Consequently, wear mechanism has changed from abrasive wear to adhesive wear with successive ECAP passes. In the EDS report, it is noticed that the transfer of iron elements from steel disc to the specimen surface increased with successive ECAP passes. This is owing to the increase in the hardness of the material with successive ECAP passes. With successive ECAP passes, oxide layer formation on the worn surface also increased. Thus, with successive ECAP passes, the intensity of oxidation wear also increased.

Figure 5 displays the SEM micrographs and EDS report of the worn surfaces of the material in different conditions, after wear test conducted at condition C4. The worn surfaces of the as-cast and the homogenized specimens were heavily damaged as displayed in Fig. 5a and b, correspondingly. Ploughing grooves were extended longitudinally towards the sliding direction. The existence of continuous wear scars and scratch marks on the worn surfaces shows the presence of abrasive wear in as-cast and homogenized specimens. In the EDS report, a large amount of aluminium and zinc traces were observed. Also, negligible traces of oxygen were observed. But, oxide layer growth was not perceived in SEM micrographs. Figure 5c and d shows the worn surface of the material after one pass ECAP at 423 K and 473 K, respectively. Comparatively shallow and narrow grooves were, observed in contrast to the as-cast and the homogenized specimens, this is owing to the increase in the hardness of the alloy after ECAP. In the EDS report, a small trace of oxygen was observed but oxide layer growth was not perceived in SEM micrographs. Adhesion of wear debris is also not observed in the SEM micrographs. Hence, it is presumed that in this condition, abrasive wear mechanism was observed in the first pass specimen processed at 423 K and 473 K, respectively. Figure 5e, f and g show the worn surface of the material after second, third and fourth passses ECAP at 473 K, respectively. It is observed that with successive ECAP passes mild wear tracks with fairly smooth surfaces were perceived. This is owing to the increase in the hardness of the material after ECAP. Sticking of the worn particles is also not perceived in the second, third and fourth pass specimens.

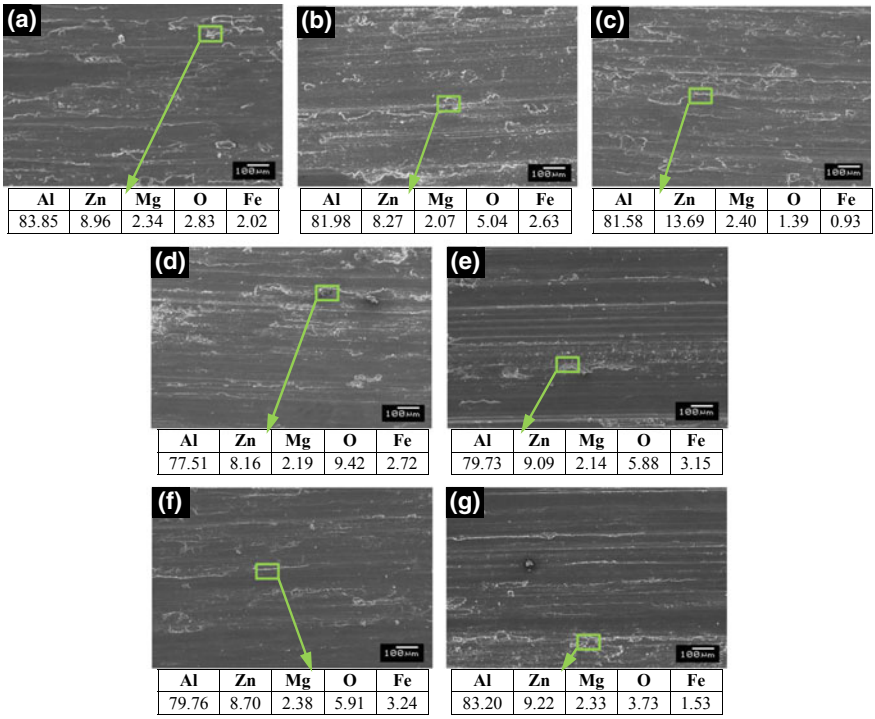

Al	Zn	Mg	O	Fe
83.85	8.96	2.34	2.83	2.02

Al	Zn	Mg	O	Fe
81.98	8.27	2.07	5.04	2.63

Al	Zn	Mg	O	Fe
81.58	13.69	2.40	1.39	0.93

Al	Zn	Mg	O	Fe
77.51	8.16	2.19	9.42	2.72

Al	Zn	Mg	O	Fe
79.73	9.09	2.14	5.88	3.15

Al	Zn	Mg	O	Fe
79.76	8.70	2.38	5.91	3.24

Al	Zn	Mg	O	Fe
83.20	9.22	2.33	3.73	1.53

Fig. 5 SEM micrographs and EDS report of the worn surfaces of the material after wear test conducted at condition C4 **a** as-cast and **b** homogenized**, c** 1 pass at 423 K, **d** 1 pass at 473 K **e** 2 pass at 473 K, **f** 3 pass at 473 K and **g** 4 pass at 473 K (EDS report is collected from the marked area)

As, in this condition of the wear test, the applied load and sliding speed both are higher, due to which worn particles might have been separated from the worn surfaces. Thus, in this condition, abrasive wear is the predominant wear mechanism perceived in ECAPed specimens. In the EDS report, a little trace of oxygen was perceived. But, its consequence on the oxide layer growth was not perceived in SEM micrographs.

4 Conclusions

Following conclusions were drawn from the current investigation.

- After ECAP, grain structure of the material was significantly refined and significant improvement in the microhardness of the alloy material was perceived.

- Wear resistance of the alloy material was enhanced with successive ECAP passes. Specimens processed at 423 K possess better wear resistance compared to the specimens processed at 473 K.
- Irrespective of the load, abrasive wear was perceived in the as-cast and homogenized specimens. Whereas in the ECAPed specimens, at lower load, along with abrasive wear; adhesive wear and oxidation wear were also perceived. At higher load, only abrasive wear was perceived.
- In the ECAP processed specimens, at lower load, transfer of iron elements from the steel disc surface to the specimen surface was perceived.

REFERENCES

1. M. Kutz, *Mechanical Engineers Handbook: Materials and Mechanical Design* (Wiley, New Jersey, 2006)
2. M.H. Shaeri, M.T. Salehi, S.H. Seyyedein, M.R. Abutalebi, J.K. Park, Mater. Des. **57**, 250 (2014)
3. L.L. Gao, X.H. Cheng, Wear **265**, 986 (2008)
4. R.Z. Valiev, T.G. Langdon, Prog. Mater Sci. **51**, 881 (2006)
5. V.M. Segal, Mater. Sci. Eng. A **271**, 322 (1999)
6. Y.T. Zehetbauer, M.J. Zhu, *Bulk Nanostructured Materials* (Wiley-VCH, Weinheim, 2009)
7. Z. Horita, T. Fujinami, M. Nemoto, T.G. Langdon, J. Mater. Process. Technol. **117**, 288 (2001)
8. I. Nikulin, R. Kaibyshev, T. Sakai, Mater. Sci. Eng. A **407**, 62 (2005)
9. Z.L. Ning, S. Guo, F.Y. Cao, G.J. Wang, Z.C. Li, J.F. Sun, J. Mater. Sci. **45**, 3023 (2010)
10. R.Z. Valiev, R.K. Islamgaliev, I.V. Alexandrov, Prog. Mater Sci. **45**, 103 (2000)
11. N. Gao, C.T. Wang, R.J.K. Wood, T.G. Langdon, J. Mater. Sci. **47**, 4779 (2012)
12. C. Xu, T.G. Langdon, Mater. Sci. Eng. A **410–411**, 398 (2005)
13. G.K. Manjunath, G.V. Preetham Kumar, K. Udaya Bhat, Trans. Indian Inst. Met. **70,** 833 (2017)
14. A. Goloborodko, O. Sitdikov, R. Kaibyshev, H. Miura, T. Sakai, Mater. Sci. Eng. A **381**, 121 (2004)
15. S. Zhang, W. Hu, R. Berghammer, G. Gottstein, Acta Mater. **58**, 6695 (2010)
16. G.K. Manjunath, G.V. Preetham Kumar, K. Udaya Bhat, AIP Conf. Proc. **1943**, 020067 (2018)
17. G.K. Manjunath, K. Udaya Bhat, G.V. Preetham Kumar, Metallogr. Microstruct. Anal. **7**, 77 (2018)
18. L.J. Zheng, H.X. Li, M.F. Hashmi, C.Q. Chen, Y. Zhang, M.G. Zeng, J. Mater. Process. Technol. **171**, 100 (2006)
19. M.I.A.E. Aal, H.S. Kim, Mater. Des. **53**, 373 (2014)
20. M.I.A.E. Aal, N.E. Mahallawy, F.A. Shehata, M.A.E. Hameed, E.Y. Yoon, H.S. Kim, Mater. Sci. Eng. A **527**, 3726 (2010)